

A Common Universality Class for the Three-Dimensional Vortex Glass and Chiral Glass?

Carsten Wengel and A. Peter Young

Department of Physics, University of California, Santa Cruz, California 95064

(June 27, 2021)

We present a Monte Carlo study of the $d = 3$ gauge glass and the XY-spin glass models in the vortex representation. We investigate the critical behavior of these models by a scaling analysis of the linear resistivity and current-voltage characteristics, both in the limits of zero and strong screening of the vortex-interactions. Without screening, both models show a glass transition at a finite temperature and, within the numerical accuracy, exhibit the *same* critical exponents: $z \approx 3.1$ and $\nu = 1.3 \pm 0.3$. With strong screening, the finite temperature glass transition is destroyed in both cases and the same exponent $\nu = 1.05 \pm 0.1$ is found at the resulting zero temperature transition.

PACS numbers: 7550.Lk, 7540.Mg, 7460.-w, 0550.+q

I. INTRODUCTION

It has been suggested^{1,2} that defects may collectively pin flux lines (vortices) in a type-II superconductor in a field, leading to a vortex glass phase with vanishing linear resistance. In many numerical studies of the vortex glass transition, a simple model called the “gauge glass” has been used.³⁻⁷ A related model is the XY-spin glass, which has been studied extensively in order to understand the magnetic ordering of a variety of magnetic compounds with random and frustrated interactions. XY-spin glasses are of special interest since they potentially exhibit two distinct kinds of ordering: spin glass ordering due to freezing of the spins, and “chiral glass” ordering due to freezing of local chiral (vortex) degrees of freedom.⁸⁻¹⁶ It has been well established^{17,18} that the spins do not have a finite temperature spin glass transition in three dimensions, whereas Kawamura^{14,16} has argued that a finite temperature chiral glass transition does occur. This intriguing claim provides one of the main motivations for the present study.

In this paper we present a comprehensive Monte Carlo study of the vortex glass transition in the gauge glass model and the chiral glass transition in the XY-spin glass in three dimensions. We consider both the situation where screening between the vortices is neglected, (which is the case in most of the earlier work) and also where there is strong screening of the vortices. We find that both with and without screening, the chiral glass and gauge glass have very similar behavior. Without screening they have a finite temperature transition with numerically very similar values for exponents, suggesting that they may lie in the same universality class. For both models, we find that screening destroys the finite temperature transition.

Our paper is organized as follows: In Sec. II we define the models under consideration. In Sec. III we discuss the quantities that we calculate and explain the finite size scaling techniques used in the analysis. In Sec. IV we present our results for the gauge glass model without screening, and briefly review results for the gauge glass

with screening that we found earlier in Ref. [7] (referred to as WY). In Sec. V we present results for the the XY-spin glass with and without screening. We summarize our results and draw our conclusions in Sec. VI.

II. THE MODELS

In the absence of screening the Hamiltonian of both the XY-spin glass and the gauge glass can be written in the *phase representation* as

$$\mathcal{H} = -J \sum_{\langle i,j \rangle} \cos(\phi_i - \phi_j - A_{ij}), \quad (1)$$

where the ϕ_i are interpreted either as phases of a superconducting order parameter (gauge glass) or as the angles of two-dimensional spins (spin glass). Here, J is the interaction strength (henceforth set to unity), and the sum is taken over all nearest neighbor sites $\langle i,j \rangle$ on a simple cubic lattice. In the case of the gauge glass, the effects of the external magnetic field and the disorder are represented by quenched vector potentials A_{ij} , taken to be uniformly distributed in the interval $[0, 2\pi]$. In the case of the $\pm J$ XY-spin glass, the random sign of the bonds between spins is represented by quenched vector potentials A_{ij} taken randomly to be 0 ($+J$) or π ($-J$).

The Hamiltonian (1) obviously possesses a $U(1)$ symmetry, i.e. the model is invariant under the transformation $\phi_i \rightarrow \phi_i + C \quad \forall i$, where C is a constant. For the gauge glass this is the only symmetry. However, for the XY-spin glass there is an additional “reflection” symmetry, $\phi_i \rightarrow -\phi_i \quad \forall i$.

It is convenient to rewrite the Hamiltonian in such a way that the chiral (vortex) variables, which are our main concern, appear explicitly. This transformation involves replacing the cosine in Eq. (1) with the periodic Gaussian Villain function, separating spin wave and vortex variables, and then performing fairly standard manipulations¹⁹⁻²¹ to obtain

$$\mathcal{H}_V = -\frac{1}{2} \sum_{i,j} G(i-j) [\mathbf{n}_i - \mathbf{b}_i] \cdot [\mathbf{n}_j - \mathbf{b}_j]. \quad (2)$$

Here, the vortex variables $\mathbf{n}_i \in \{0, \pm 1, \pm 2, \dots\}$ sit on the links of the *dual* lattice (which is also a simple cubic lattice here), $G(i-j)$ is the lattice Green's function

$$G(i-j) = \frac{(2\pi)^2}{L^3} \sum_{\mathbf{k} \neq 0} \frac{1 - \exp[i \mathbf{k} \cdot (\mathbf{r}_i - \mathbf{r}_j)]}{2 \sum_{n=1}^d [1 - \cos(k_n)]}, \quad (3)$$

(with $d = 3$), and the \mathbf{b}_i are quenched fluxes given by $(1/2\pi)$ times the directed sum of the quenched vector potential A_{ij} on the original lattice surrounding the link on the dual lattice on which \mathbf{b}_i lies. Due to periodic boundary conditions, we have the global constraints $\sum_i \mathbf{b}_i = \sum_i \mathbf{n}_i = 0$. There are also the *local* constraints, $[\nabla \cdot \mathbf{n}]_i = [\nabla \cdot \mathbf{b}]_i = 0$, where the latter just follows trivially from the definition of \mathbf{b}_i as a lattice curl.

Since the Hamiltonian only depends on $\mathbf{n}_i - \mathbf{b}_i$ it is convenient to discuss the distribution of the quenched fluxes when all the weight is shifted into the interval²² $0 \leq b_i^\alpha < 1$ (where α is a Cartesian component). For the gauge glass model, the distribution of the shifted b^α is uniform, i.e.

$$P(b^\alpha) = 1 \quad (0 \leq b^\alpha < 1) \\ = 0 \quad (\text{otherwise}), \quad (4)$$

while for the $\pm J$ spin glass the shifted b^α have a bi-modal distribution with equal weight at 0 (corresponding to an unfrustrated square on the original lattice) and $1/2$ (corresponding to a frustrated square):

$$P(b^\alpha) = \frac{1}{2} \left(\delta(b^\alpha) + \delta(b^\alpha - \frac{1}{2}) \right). \quad (5)$$

Recent work on the gauge glass model and on the XY-spin glass have investigated the role of screening of the vortex-vortex interactions, which is a relevant perturbation near the critical temperature^{2,6}. It was found by Wengel and Young (WY)⁷ and Ref. [6], that the vortex glass phase vanishes when strong screening is included in the $d = 3$ gauge glass model, and subsequent work by Kawamura and Li¹⁶ found the same effect for the chiral glass transition. We therefore also discuss the effects of screening here.

In the vortex representation, the Hamiltonian is still represented by Eq. (2) but now the interaction $G(i-j)$ has the screened form

$$G(i-j) = \frac{(2\pi)^2}{L^3} \sum_{\mathbf{k} \neq 0} \frac{1 - \exp[i \mathbf{k} \cdot (\mathbf{r}_i - \mathbf{r}_j)]}{2 \sum_{n=1}^d [1 - \cos(k_n)] + \lambda_0^{-2}}, \quad (6)$$

where λ_0 is a bare screening length. Note that in the long wavelength limit, the denominator is just $k^2 + \lambda_0^{-2}$.

In the simulations presented here, we consider just two cases: (i) $\lambda = \infty$, where there is no screening and the interactions between the vortices are long range, and (ii) $\lambda \rightarrow 0$, where there is strong screening. In the latter case $G(r \neq 0) = (2\pi\lambda_0)^2$ with corrections which are exponentially small, i. e., of order $\exp(-r/\lambda_0)$. Because

$\sum_i (\mathbf{n}_i - \mathbf{b}_i) = 0$ we can always add a constant to $G(r)$ for all r without affecting the results. We therefore add $-(2\pi\lambda_0)^2$, as a result of which the only interaction is on-site, and then divide the interaction by $(2\pi\lambda_0)^2$ to have a well defined limit for $\lambda_0 \rightarrow 0$. The resulting Hamiltonian then has the very simple form

$$\mathcal{H}_V = \frac{1}{2} \sum_i (\mathbf{n}_i - \mathbf{b}_i)^2 \quad (\lambda_0 \rightarrow 0). \quad (7)$$

Note²³, however, that \mathcal{H}_V is not trivial because the local constraint $[\nabla \cdot \mathbf{n}]_i = 0$ effectively generates interactions between the \mathbf{n}_i .

To summarize, we study four models in this paper:

1. The gauge glass in the absence of screening. The Hamiltonian is given by Eq. (2) where the $G(i-j)$ are given by Eq. (3), and the distribution of the fluxes (shifted²² into the interval from 0 to 1) is given by Eq. (4).
2. The gauge glass with strong screening. The Hamiltonian is given by Eq. (7) in which the distribution of the (shifted) fluxes is given by Eq. (4).
3. The chiral glass (i.e. vortex degrees of freedom in the XY-spin glass) in the absence of screening. The Hamiltonian is given by Eq. (2) where the $G(i-j)$ are given by Eq. (3), and the distribution of the (shifted) fluxes is given by Eq. (5).
4. The chiral glass with strong screening. The Hamiltonian is given by Eq. (7) in which the distribution of the (shifted) fluxes is given by Eq. (5).

III. DATA ANALYSIS

We simulate the Hamiltonians in Eq. (2) and (7) on simple cubic lattices with $N = L^3$ sites where $4 \leq L \leq 12$. Periodic boundary conditions are imposed. We start with configurations with all $\mathbf{n}_i = 0$, which clearly satisfies the constraints, and a Monte Carlo move consists of trying to create a loop of four vortices around a square. This trial state is accepted with probability $1/(1 + \exp(\beta \Delta E))$, where ΔE is the change of energy and $\beta = 1/T$. Each time a loop is formed it generates a voltage $\Delta Q = \pm 1$ perpendicular to its plane, the sign depending on the orientation of the loop. This leads to a net voltage⁵

$$V(t) = \frac{h}{2e} I^V(t) \quad \text{with} \quad I^V(t) = \frac{1}{L \Delta t} \Delta Q(t), \quad (8)$$

where I^V is the vortex-current and t denotes Monte Carlo "time" incremented by Δt for each attempted Monte Carlo move. We will work in units where $h/(2e) = 1$, and we set $\Delta t = 1/(3N)$ so that an attempt is made to create or destroy one vortex loop per square in each direction, on average, per unit time.

The linear resistivity can be calculated from the voltage fluctuations via the Kubo formula²⁴

$$\rho_{\text{lin}} = \frac{1}{2T} \sum_{t=-\infty}^{\infty} \Delta t \langle V(t)V(0) \rangle. \quad (9)$$

Here, $\langle \dots \rangle$ denotes the combined thermal and disorder average. Near a second order phase transition the linear resistivity obeys the scaling law²

$$\rho_{\text{lin}}(T, L) = L^{-(2-d+z)} \tilde{\rho}(L^{1/\nu}(T - T_c)), \quad (10)$$

where ξ is the correlation length exponent, i.e.,

$$\xi \sim (T - T_c)^{-\nu}, \quad (11)$$

z is the dynamical exponent, and $\tilde{\rho}$ is a scaling function. At the critical temperature, $\tilde{\rho}$ becomes a constant and therefore $\rho_{\text{lin}}(T_c, L) \sim L^{-(2-d+z)}$. If we plot the ratio of ρ_{lin} for different system sizes against T , then

$$\frac{\ln[\rho_{\text{lin}}(L)/\rho_{\text{lin}}(L')]}{\ln[L/L']} = d - 2 - z \quad \text{at } T_c, \quad (12)$$

i.e., all curves for different pairs (L, L') should intersect and one can read off the values of T_c and z . We will refer to this kind of data plot as the ‘‘intersection method’’. With the values of T_c and z determined by the intersection method we can then use a scaling plot according to Eq. (10) to obtain the value of ν .

In the case of strong screening we find a zero temperature transition and a plot according to Eq. (10) to determine ν does not work, since $z = \infty$ because there is activated dynamical scaling at the $T = 0$ transition. However, one can still obtain static exponents by measuring the voltage generated by a finite external current, i. e., by I - V characteristics. In real superconductors, transport currents generate a non-uniform magnetic field because of Ampère’s law, $\vec{\nabla} \times \mathbf{B} = \mathbf{J}$. It is inconvenient to simulate a non-uniform system, so instead we effectively assume that the current is the same everywhere so *each* vortex feels a Lorentz force $\mathbf{n}_i \times \mathbf{J}$. The scaling behavior of the response to such a perturbation should be the same as that derived earlier for response to an actual transport current². We can therefore use this approach to determine critical exponents, which is our objective. The Lorentz force biases the moves and sets up a net flow of vortices perpendicular to the current, whose time average gives the voltage according to⁵ Eq. (8).

To analyze our data we need to understand the scaling behavior of the I - V -curves near a second order phase transition. The scaling theory gives^{2,5}

$$T \frac{E}{J} \frac{\tau}{\xi^{d-2}} = g \left(\frac{J\xi^{d-1}}{T} \right), \quad (13)$$

where E is the electric field, J the current density, τ a relaxation time, and g is a scaling function. At a zero temperature transition one has

$$\xi \sim T^{-\nu}, \quad (14)$$

so, in three dimensions, Eq. (13) becomes

$$T^{1+\nu} \frac{E}{J} \tau = g \left(\frac{J}{T^{1+2\nu}} \right). \quad (15)$$

From this equation we can see that the current scale, J_{NL} , at which nonlinear behavior sets in varies with T as $J_{\text{NL}} \sim T^{1+2\nu}$. Since the linear resistivity is defined by

$$\rho_{\text{lin}} = \lim_{J \rightarrow 0} \frac{E}{J}, \quad (16)$$

and $g(0)$ can be taken to be unity, we can write

$$\frac{E}{J\rho_{\text{lin}}} = g \left(\frac{J}{T^{1+2\nu}} \right). \quad (17)$$

Furthermore, we expect that near the $T = 0$ transition, long time dynamics will be governed by activation over barriers. Hence we expect

$$T^{1+\nu} \rho_{\text{lin}} = \frac{1}{\tau} = A \exp(-\Delta E(T)/T), \quad (18)$$

where ΔE is the typical barrier that a vortex has to cross to move a distance ξ . One can define a barrier height exponent ψ by $\Delta E \sim \xi^\psi \sim T^{-\psi\nu}$ in terms of which

$$T^{1+\nu} \rho_{\text{lin}} = A \exp(-C/T^{1+\psi\nu}). \quad (19)$$

We are able to obtain a rough estimate for ψ from our data of the linear resistivity.

In a finite system, the I - V characteristics will also depend on the ratio L/ξ . One can generalize the scaling function, Eq. (17), to account for finite size effects as follows:

$$\frac{E}{J\rho_{\text{lin}}} = \tilde{g} \left(\frac{J}{T^{1+2\nu}}, L^{1/\nu} T \right). \quad (20)$$

Now we are left with a rather complicated scaling function since it depends on two variables. To simplify the analysis we first estimate ν by determining the current where $E/(J\rho_{\text{lin}}) = 2$, at which point non-linear effects start to become significant. Denoting these values of J by J_{NL} , then, from Eq. (20), it follows that

$$\frac{J_{\text{NL}}}{T^{1+2\nu}} = \tilde{g} \left(L^{1/\nu} T \right), \quad (21)$$

where \tilde{g} is another function. Hence we determine ν by requiring that the scaling in Eq. (21) is satisfied. We then collect data for sizes and temperatures such that $L^{1/\nu} T$ is constant. The scaling function in Eq. (20) then only depends on *one* variable, and so data for $E/J\rho_{\text{lin}}$ for different sizes should scale when plotted against $J/T^{1+2\nu}$, with the *same* value of ν as obtained from the scaling of J_{NL} . We find, in fact, that the results are only weakly dependent on the second argument of Eq. (20).

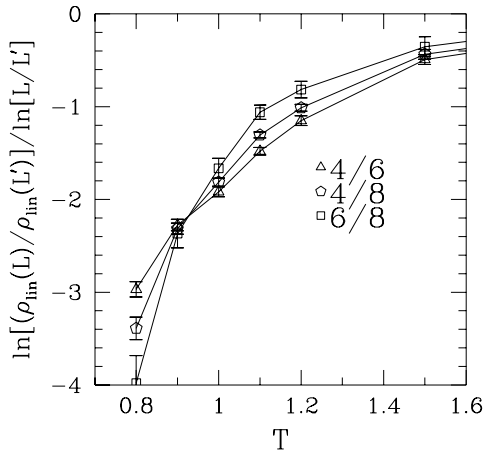


FIG. 1. Plot of $\ln[\rho_{\text{lin}}(L)/\rho_{\text{lin}}(L')]/\ln[L/L']$ versus T for the gauge glass with $\lambda_0 \rightarrow \infty$. The curves intersect at $T_c = 0.93 \pm 0.05$. At the intersection point, the y -value is approximately -2.2 , corresponding to $z_{\text{GG}} \approx 3.2$.

IV. RESULTS FOR THE GAUGE GLASS

In this section we consider the critical behavior of the gauge glass model with and without screening. Recall that the distribution of the (shifted) fluxes is given by Eq. (4).

A. No screening, $\lambda_0 \rightarrow \infty$

For the gauge glass with no screening we have measured the linear resistivity ρ_{lin} as a function of temperature. In Fig. 1 we show data of ρ_{lin} plotted according to the intersection method vs. T for sizes $L = 4, 6, 8$. We were not able to include data from $L = 10$ into this plot since we could not equilibrate the systems down to the lowest temperatures ($T = 0.8, 0.9$). All curves intersect at about $T = 0.93 \pm 0.05$ indicating a phase transition to a vortex glass. The corresponding y -axis value at the intersection point is $1 - z \approx -2.2$, therefore $z_{\text{GG}} \approx 3.2$. Having established these values, we tried a scaling plot according to Eq. (10) and the result is shown in Fig. 2. Best scaling was achieved with $T_c = 0.93$, $z_{\text{GG}} = 3$ and $\nu_{\text{GG}} = 1.3 \pm 0.3$. Only far away from the transition point does one observe deviations from scaling, which is expected for such small sizes and high temperatures, but the overall scaling works quite well.

It is interesting to compare this result with earlier Monte Carlo simulations of the gauge glass without screening in the phase representation by Reger et al.⁴ These authors did a finite size scaling analysis of static quantities which indicated a finite temperature transition, but they could not completely rule out the possibility that the lower critical dimension is $d_l \simeq 3$. The clear

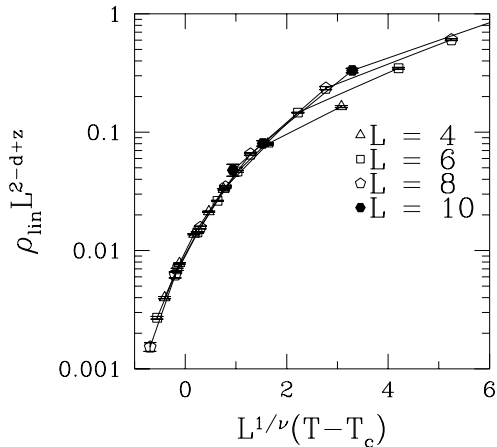


FIG. 2. Scaling plot of the lineage resistivity for the gauge glass with $\lambda_0 \rightarrow \infty$. Using $T_c = 0.93$ and $z_{\text{GG}} = 3$ from Fig. 1 we obtain $\nu_{\text{GG}} = 1.3 \pm 0.3$.

intersection of the data in Fig. 1, however, strongly confirms the notion that there is a finite temperature transition in the three-dimensional gauge glass model, and hence $d_l < 3$. Additionally, our correlation length exponent ν_{GG} agrees well with the estimate given by Reger et al.⁴, $\nu_{\text{GG}} = 1.3 \pm 0.4$. There is, however, a considerable difference between our estimate of the dynamic critical exponent $z \approx 3.1$ and theirs, $z = 4.7 \pm 0.7$. It is possible, though, that the *dynamical* universality classes of the models in the phase and vortex representations may be different, even though the static behavior is the same. If so, there is no contradiction in the results.

B. Strong Screening, $\lambda_0 \rightarrow 0$

In this paragraph we review quickly the results for the gauge glass model with strong screening found earlier by WY, in order to compare them in the next section with our data for the $d = 3$ XY-spin glass model with screening. As shown by WY the vortex glass transition in the gauge glass is destroyed by screening of the vortex-interactions. The main indication for the lack of a transition at finite T was the absence of an intersection if the resistivity was plotted according to the intersection method. A scaling plot of the current-voltage characteristics for different temperatures and sizes also revealed $T_c = 0$ and $\nu_{\text{GG}} = 1.05 \pm 0.1$. Finally, the barrier exponent ψ , as defined in Eq. (19), was determined to be close to zero, so the conclusion was drawn that energy barriers diverge only weakly, possibly logarithmically, as one approaches the zero temperature transition.

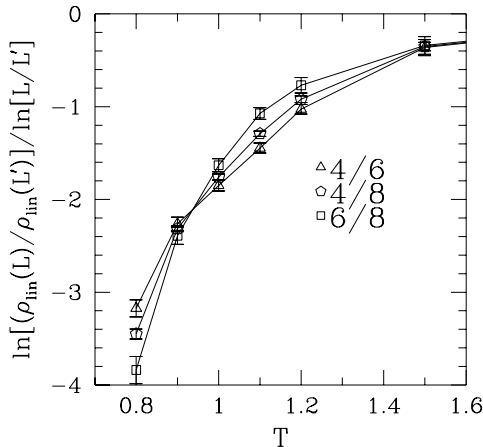


FIG. 3. Plot of $\ln[\rho_{\text{lin}}(L)/\rho_{\text{lin}}(L')]/\ln[L/L']$ versus T for the $\pm J$ XY-spin glass and $\lambda_0 \rightarrow \infty$. The curves intersect at $T_c = 0.94 \pm 0.05$. At the intersection point, the y -value is approximately -2.2, corresponding to $z_{\text{CG}} \simeq 3.2$.

V. RESULTS FOR THE $\pm J$ XY-SPIN GLASS

Recall that the only difference between the $\pm J$ XY-spin glass and the gauge glass discussed in the last section is that the distribution of shifted fluxes is given by Eq. (5) rather than by Eq. (4).

A. No screening, $\lambda_0 \rightarrow \infty$

As already discussed in the introduction, the $\pm J$ XY-spin glass is known to have no finite-temperature transition to an ordered state below four dimensions¹⁷. For the $d = 3, \pm J$ model one can, however, identify a chiral glass transition in Monte Carlo simulations due to freezing out of the discrete degrees of freedom, as has been done by Kawamura et al.¹⁴ The associated chiral glass exponents estimated in the phase representation with periodic boundary conditions¹⁴ are $\nu_{\text{CG}} = 1.5 \pm 0.3$ and $\eta_{\text{CG}} = -0.4 \pm 0.2$. Subsequent work with free boundary conditions¹⁶ finds similar values, $\nu_{\text{CG}} = 1.3 \pm 0.2$ and $\eta_{\text{CG}} = -0.2 \pm 0.2$.

Figure 3 displays a plot of our data for ρ_{lin} according to the intersection method vs. T for the XY-spin glass. One observes, very similarly to Fig. 1, an intersection point at $T = 0.93 \pm 0.05$ and a dynamic critical exponent $z_{\text{CG}} \approx 3.2$. Also, the scaling plot of ρ_{lin} shows best results with almost the same values as in the long range gauge glass case, namely $T_c = 0.93$, $z_{\text{CG}} = 3.1$ and $\nu_{\text{CG}} = 1.3 \pm 0.3$. This result indicates a finite-temperature transition into a chiral glass state for the $d = 3$ XY-spin glass and thereby confirms Monte Carlo results performed in the phase representation.¹⁴ Very surprisingly, we find that our data for the linear resistivity is

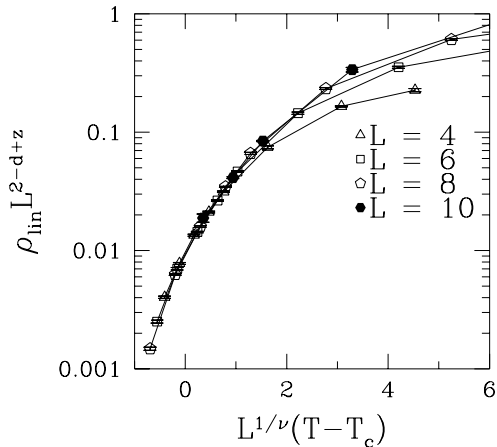


FIG. 4. Scaling plot of the lineage resistivity for the $\pm J$ XY-spin glass with $\lambda_0 \rightarrow \infty$. Using $T_c = 0.94$ and $z_{\text{CG}} = 3.1$ from Fig. (3) we obtain $\nu_{\text{CG}} = 1.3 \pm 0.3$.

virtually indistinguishable from the corresponding measurements of the gauge glass model. We observe a maximum deviations of 1.5σ . We will come back to this in the last section.

B. Strong screening, $\lambda_0 \rightarrow 0$

In Fig. 5 we show the linear resistivity plotted according to the intersection method vs. T . One can see, that there is no apparent intersection over the entire temperature range that we have been able to simulate, i. e., down to $T = 0.07$ for $L \leq 8$ and $T = 0.1$ for $L \leq 12$. At high temperatures all curves merge, since the correlation length becomes shorter than the system size and the data of ρ_{lin} for different sizes are the same. This rules out a transition down to $1/5$ of the critical temperature of the system without disorder, $T_c = 0.331$ (see WY), and therefore strongly suggests the absence of a chiral glass transition at finite temperature, in agreement with work by Kawamura and Li.¹⁶

Next we studied the current-voltage characteristics of our model in order to determine ν . Figure 6 shows a scaling plot of different I - V curves according to Eq. (20). From the scaling of the nonlinear current J_{NL} we estimated $\nu_{\text{CG}} = 1$, and then chose sizes and temperatures for the data in Fig. 6 such that $L^{1/\nu_{\text{CG}}}T = \text{const.}$, and hence the second argument in Eq. (20), remained roughly constant. The data is seen to scale very well with $T_c = 0$ and $\nu_{\text{CG}} = 1.05 \pm 0.1$. We also attempted scaling our data with an appropriate scaling function for finite T_c , and found that scaling works only moderately well with $T_c = 0.04$ and $\nu_{\text{CG}} = 1.05$. We, therefore, conclude that the transition is very likely to occur at $T_c = 0$, but we cannot completely rule out a finite, though extremely small T_c .

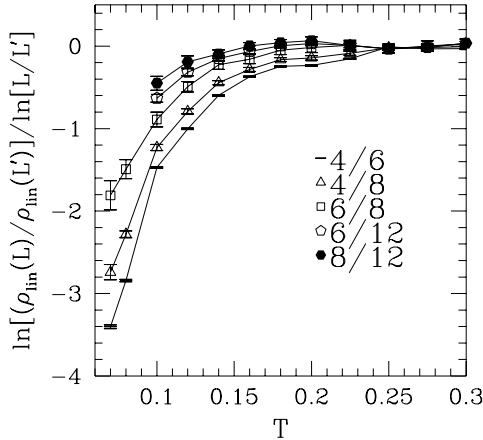


FIG. 5. Plot of $\ln[\rho_{\text{lin}}(L)/\rho_{\text{lin}}(L')]/\ln[L/L']$ vs. T for the XY-spin glass model with $\lambda_0 \rightarrow 0$. In contrast to Fig. 3 there is no intersection over the entire temperature range, indicating the absence of a phase transition into a chiral glass.

We also determined the barrier exponent ψ by plotting $T^2\rho_{\text{lin}}$ over $1/T$ as was done in Fig. 4 of WY for the gauge glass. The data for $L = 12$ follows almost a straight line indicating Arrhenius behavior and therefore $\psi \simeq 0$. As in the gauge glass case one has to be careful though, since such an estimate does not allow for finite-size corrections and is only observed over a small range of temperatures. It is also possible, that we only measure an effective exponent and the true value of ψ changes as one gets closer to $T = 0$. In any case, $\psi \simeq 0$ would suggest, that barriers increase only very slowly, possibly logarithmically, as one approaches the zero temperature chiral glass transition.

Again it is interesting to compare these results with those obtained by WY for the gauge glass with screening: they agree perfectly with in the errors, namely $T_c = 0$, $\nu_{\text{CG}} = 1.05$ and $\psi \simeq 0$, as described in Sec. IV B. Not only do the final estimates of the exponents for the gauge glass and $\pm J$ XY-spin glass agree but also, as in the case without screening, the individual numerical values of ρ_{lin} and data from the I - V characteristics all agree within the errorbars, the maximum discrepancy being 1.5σ .

VI. SUMMARY AND DISCUSSION

In this article we have presented a Monte Carlo study of the gauge glass model and the chiral glass transition in the XY-spin glass model with and without screening, in the vortex representation. We have computed dynamic quantities such as the linear resistivity and current-voltage characteristics and used finite-size scaling techniques to extract the critical behavior of these models.

Our main results are:

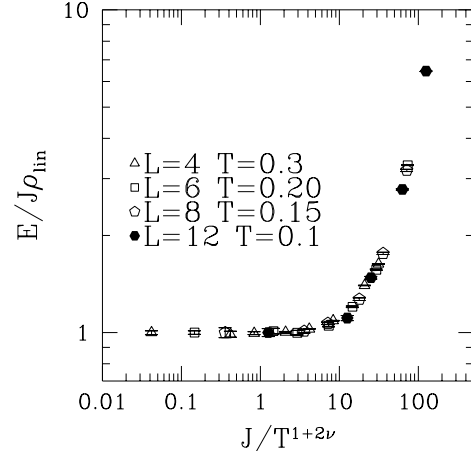


FIG. 6. Scaling plot of the I - V characteristics with $T_c = 0$ and $\nu_{\text{CG}} = 1.05 \pm 0.1$, according to Eq. (20), choosing sizes and temperatures such that $L^{1/\nu_{\text{CG}}}T$ is roughly constant.

Screening	T_c	ν	z	ψ
$\lambda_0 \rightarrow \infty$	0.94 ± 0.05	1.3 ± 0.3	≈ 3.1	n/a
$\lambda_0 \rightarrow 0$	0	1.05 ± 0.1	∞	$\simeq 0$

TABLE I. Critical temperatures and exponents of the presumed common universality class of the gauge glass and the chiral glass in $d = 3$. ν is the correlation length exponent, z is the dynamical exponent, and ψ is the barrier exponent for the $T = 0$ transition in the strong screening limit.

1. In the absence of screening there is a finite temperature transition in both cases with numerically indistinguishable exponents given in Table. 1.
2. In the presence of strong screening, there is a transition at zero temperature in both cases. The correlation length exponent is the same for the two models, as shown in Table 1.
3. Not only do the gauge glass transition and the chiral transition in the XY-spin glass model appear numerically to be in the same universality class, but even the individual data points for the current-voltage characteristics are virtually indistinguishable.

Earlier work which provided evidence for a finite temperature chiral glass transition^{14,16} used the phase representation and constructed the chiralities (vortices) indirectly from the spin configurations. This is only sensible at moderate to low temperatures where correlations in the angles of nearest neighbor spins become significant. Our work is the first which demonstrates the existence of a chiral glass transition using the vortex representation. In our model vortices are well defined at *all* temperatures

and so we expect that the region over which scaling behavior is obtained will be larger than in the earlier work in the phase representation. We therefore feel that our results make the existence of the chiral glass transition more convincing.

There is also support in two dimensions for the idea that the chiral glass and gauge glass transitions are in the same universality class since in both cases one finds^{12,11,5,6,15} $T_c = 0$ and $\nu \approx 2$.

However it is unclear to us theoretically why the gauge glass and the chiral glass transition in the $\pm J$ XY-spin glass *should* be in the same universality class. For the XY-spin glass, the important low energy states are those where $n_i^\alpha - b_i^\alpha = 0$ on links where $b_i^\alpha = 0$ (corresponding to an unfrustrated square on the original lattice) and $n_i^\alpha - b_i^\alpha = \pm 1/2$ on links where $b_i^\alpha = 1/2$. Thus, as first noted by Villain,⁸ one has a random Ising model with long range antiferromagnetic interactions,

$$\mathcal{H} = -\frac{1}{4} \sum_{\langle i,j \rangle} G(i-j) \epsilon_i \epsilon_j S_i S_j, \quad (22)$$

where the ϵ_i are quenched variables taking values 0 or 1, and the S_i are statistical Ising-like variables which take values ± 1 . For the gauge glass one cannot make an analogous transformation and Eq. (2) corresponds to an Ising model *in a random field*, which is not expected to be in the same universality class as Eq. (22). We do not, therefore, understand why the numerical values of the exponents are the same within the uncertainties. Even more surprising is that the individual I-V values for the two models are virtually indistinguishable. We would expect there to be a more clearly visible difference in other properties. Perhaps for some reason, the random field aspect of the gauge glass is irrelevant, or perhaps the critical behaviors of the two models just happen by coincidence to be very close. It would be interesting to check our results by studying both models by alternative techniques such as domain wall renormalization group methods.

The correlation length exponent for the unscreened models is also very similar to that of the Ising spin glass²⁵ with short range interactions. Again, it is not obvious to us why this should be the case. While the model in Eq. (22) has Ising variables, and the ingredients of randomness and frustration necessary for a spin glass, it also has long range interactions, unlike the Ising spin glass.

Finally, it is noteworthy, that earlier results for the gauge glass⁶ indicated that the universality class changes (and hence T_c becomes zero) for any non-infinite value of the bare screening length. By contrast, Kawamura and Li¹⁶ have argued that the transition in the chiral glass persists down to a finite value of λ_0 . It would, therefore, also be interesting to study these models with an intermediate range of screening in the vortex representation.

ACKNOWLEDGMENTS

We wish to thank Hemant Bokil, Muriel Ney-Nifle and Christian Pich for useful discussions. This work has been supported by NSF grant DMR 94-11964. The work of CW has also been supported in part by a fellowship of the German Academic Exchange Service (Doktorandenstipendium HSP II/AUFE). We would like to thank the Maui High Performance Computing Center for an allocation of computer time.

-
- ¹ M. P. A. Fisher, Phys. Rev. Lett. **62**, 1415, 1989.
 - ² D. S. Fisher, M. P. A. Fisher, and D. A. Huse, Phys. Rev. B **43**, 130 (1991).
 - ³ M. P. A. Fisher, T. A. Tokuyasu and A. P. Young, Phys. Rev. Lett. **66**, 2931 (1991).
 - ⁴ J. D. Reger, T. A. Tokuyasu, A. P. Young and M. P. A. Fisher, Phys. Rev. B **44**, 7147 (1991).
 - ⁵ R. A. Hyman, M. Wallin, M. P. A. Fisher, S. M. Girvin and A. P. Young, Phys. Rev. B **51**, 15304 (1995).
 - ⁶ H. S. Bokil and A. P. Young, Phys. Rev. Lett. **74**, 3021 (1995).
 - ⁷ C. Wengel and A. P. Young, Phys. Rev. B **10**, R6869 (1996), referred to as WY.
 - ⁸ J. Villain, J. Phys. C **10**, 4793 (1977); J. Phys. C **11**, 745 (1978).
 - ⁹ H. Kawamura and M. Tanemura, J. Phys. Soc. Japan **54**, 4479 (1985); Phys. Rev. B **36**, 7177 (1987).
 - ¹⁰ D. A. Huse and H. S. Seung, Phys. Rev. B **42**, 1059 (1990).
 - ¹¹ P. Ray and M. A. Moore, Phys. Rev. B **45**, 5361 (1992).
 - ¹² H. Kawamura and M. Tanemura, J. Phys. Soc. Jpn. **60**, 608 (1991).
 - ¹³ H. Kawamura, Phys. Rev. Lett. **68**, 3785 (1992).
 - ¹⁴ H. Kawamura, Phys. Rev. B **51**, 12398 (1995). H. Kawamura and M. S. Li, Phys. Rev. B **54**, 619 (1996).
 - ¹⁵ H. S. Bokil and A. P. Young, J. Phys. A **29**, L89 (1996).
 - ¹⁶ H. Kawamura and M. S. Li, preprint cond-mat/9702157.
 - ¹⁷ S. Jain and A. P. Young, J. Phys. C **19**, 3913 (1986). B. W. Morris, S. G. Colborne, M. A. Moore, A. J. Bray and J. Canisius, *ibid.* **19**, 1157 (1986).
 - ¹⁸ S. Jain, J. Phys. A **29**, L385 (1996).
 - ¹⁹ J. V. José, L. P. Kadanoff, S. K. Kirkpatrick, and D. R. Nelson, Phys. Rev. B **16**, 1217 (1977).
 - ²⁰ C. Dasgupta and B. I. Halperin, Phys. Rev. Lett. **47**, 1556 (1981).
 - ²¹ H. Kleinert, *Gauge Fields in Condensed Matter*, (World Scientific, Singapore, 1989); see e.g. §7.1.
 - ²² Note that shifting the fluxes \mathbf{b}_i and compensating by shifting the vortex variables \mathbf{n}_i in Eqs. (2) and (7), violates the neutrality condition $\sum_i \mathbf{n}_i = 0$. Hence the distributions of the shifted fluxes, given in Eqs. (4) and (5), are for intuitive purposes only. In the simulations, the fluxes were determined from the directed sum of the four vector potentials (chosen with the appropriate distribution) around

the corresponding loop of the original lattice.

²³ Note also that without disorder (i. e., all $\mathbf{b}_i = 0$) this model is just a dual representation of the XY -model^{20,21} (with the Villain potential), in which the temperature scale has been inverted.

²⁴ The Kubo formula is exact for discrete time MC dynamics, provided the sum is made symmetrical about $t = 0$. See A. P. Young, in *Proceedings of the Ray Orbach Inauguration Symposium* (World Scientific, Singapore, 1994).

²⁵ See e.g. N. Kawashima and A. P. Young, *Phys. Rev. B* **53**, R484 (1996) and references therein.